Applied **CLAY** Science

Modelling of long-term diffusion–reaction in a bentonite barrier for radioactive waste confinement

G. Montes-H [a],*, N. Marty [a], B. Fritz [a], A. Clement [a], N. Michau [b]

[a] *UMR 7517 ULP-CNRS, CGS, 1 rue Blessig, F-67084 Strasbourg, France*
[b] *ANDRA, 1/7 rue Jean Monnet, F-92298 Châtenay-Malabry Cedex, France*

Abstract

Bentonites have been proposed as buffer material for barriers in geological disposal facilities for radioactive waste. This material is expected to fill up by swelling the void between the canisters containing the waste and the surrounding ground. However, the bentonite barriers may be submitted to changes of humidity, temperature variation, fluid interaction, mass transport, etc. This could modify the physico-chemical performance of the barrier, mainly on the interface with the steel container and with the geological barrier. The engineered barrier development necessitates thus the study of the physico-chemical stability of its mineral component as a function of time under the conditions of the repository in the long-term.

The purpose of the present study was two-fold. Firstly, it was hoped to simulate the chemical transformations (geochemical and cation exchange reactions) coupled with diffusion of chemical-elements into the engineered barrier under repository conditions by applying a thermokinetic hydrochemical code (KIRMAT: Kinetic Reactions and Mass transport).

Secondly, it was hoped to apply a simplified method to estimate the swelling capacity evolution by a volume balance in the fluid-saturated engineered barrier, considering that the decay of swelling capacity is directly proportional on the volume of transformed montmorillonite and, taking into account that it may be partially compensated by the volume of neo-formed swelling clays.

The system modelled herein was considered to consist of 1-m thick zone of water-saturated engineered barrier. This non-equilibrated system was placed in contact with a geological fluid on one side, which was then allowed to diffuse into the barrier, while the other side was kept in contact with a source of metallic iron. Reducing initial conditions ($P_{O_2} \cong 0$; Eh = − 200 mV) and a constant reaction temperature (100 °C) were considered.

The results showed that the EB in contact with the geological fluid was highly transformed after 10,000 years, whereas the most significant chemical processes were illitization, cation exchange and saponization, extending up to 20 cm into the EB. Chemical transformations of minor importance in the EB were identified as well, such as a neo-formation of silicates (quartz, cristobalite), anhydrite, laumontite, magnetite and chlorite in the system.

A simplified method based on volume balance showed that the swelling capacity of the bentonite barrier is slightly affected after 10,000 years of diffusion–reaction (D close to 1) because the volume of neo-formed swelling-clays is almost directly

* Corresponding author. Fax: +33 390240402.
  E-mail addresses: montes@illite.u-strasbg.fr, german_montes@hotmail.com (G. Montes-H).

proportional to the volume of transformed Na/Ca-montmorillonite, except for a strong illitization and/or neo-formation of non-swelling clays. In the present study, this simple approach predicted that the decay of swelling capacity of the engineered barrier is drastically affected close to the geological barrier-engineered barrier interface. Out this zone the swelling capacity decay lies between 5% and 11%.

1. Introduction

The radioactive waste confinement in deep geological layers of impermeable clay has been proposed in the last decades. Vitrified waste is laid in canisters in the middle of a gallery dug in the clay formations. In order to protect the canisters from water intrusion, and to eventually trap released radioelements, waste-forms will be isolated from the surrounding geological media by two barriers: (a) the steel canister, and (b) an engineered backfill barrier system. This backfill barrier will be essentially composed of compacted clay blocks because of the hydrodynamic and surface properties of clay materials. In addition, the swelling characteristics of the buffer material are expected to fill up the void between the canisters containing the waste and the surrounding ground, and to build a better impermeable zone around high-level radioactive wastes. This role is called "self-sealing" (Komine, 2004; Komine and Ogata, 2003).

MX80 bentonite (bentonite of Wyoming) contains approximately 85% of Na/Ca-montmorillonite (Na/Ca=1.8) and 15% of accessory minerals (Sauzéat et al., 2001). The dominant presence of Na/Ca-montmorillonite in this clay mineral could cause it to perform exceptionally well as an engineered barrier for a radioactive waste repository because of its swelling properties (see Fig. 1). However, the Na/Ca-montmorillonite could be transformed to other clay minerals as a function of time under repository conditions. Previous modelling studies based on the hydrolysis reactions have shown that the Na/Ca-montmorillonite-to-Ca-montmorillonite conversion is the most significant chemical transformation (swelling clays). In fact, this chemical process appears to be a simple cation exchange into the engineered barrier. A minimal neo-formation of non-swelling clays (chlorites and illite) was also identified in simulations as a potential chemical transformation in the bentonite barrier (Kluska et al., 2002; Montes-H et al., 2005).
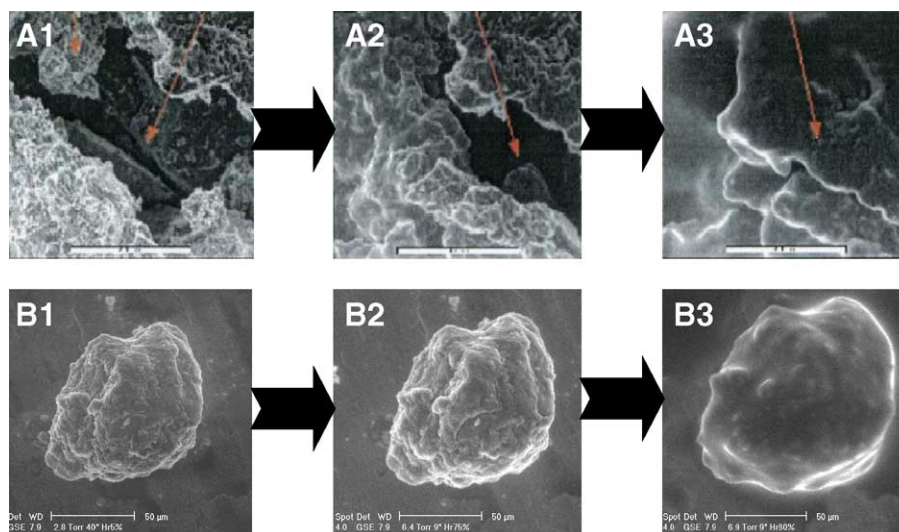

Fig. 1. Swelling behaviour of montmorillonite in a bentonite-buffer material. (A) Filling of a macropore by swelling (Komine and Ogata, 2003), (B) swelling of a bentonite aggregate (Montes-H et al., 2003b). (1) Initial state, (2) during hydration, (3) water oversaturation beginning.

The purpose of the present study was two-fold. Firstly, it was hoped to simulate the chemical transformations (geochemical and cation exchange reactions) coupled with the chemical-elements diffusion into the engineered barrier under repository conditions by applying a thermokinetic hydrochemical code (KIRMAT: Kinetic Reactions and Mass transport) (Gérard et al., 1998).

Secondly, it was hoped to apply a simplified method to estimate the swelling capacity evolution by a volume balance in the fluid-saturated engineered barrier, considering that the decay of swelling capacity is directly proportional on the volume of transformed montmorillonite and, taking into account that it may be partially compensated by the volume of neo-formed swelling clays (Montes-H et al., 2005).

The system modelled herein was considered to consist of 1-m thick zone of water-saturated engineered barrier. This non-equilibrated system (pure water as interacting fluid) was placed in contact with a geological fluid on one side, which was then allowed to diffuse into the barrier, while the other side was kept in contact with a source of metallic iron. This configuration represented the contact of an engineered barrier (EB) with a geological barrier (GB) and with an iron container (C) in a geological disposal facility for radioactive wastes (Fig. 2).

A grid spacing of 5 cm was used for all the calculations reported, i.e. the thick zone of the engineered barrier was divided into 20 grids.

Reducing initial conditions ($P_{O_2} \cong 0$; Eh $= -200$ mV) and a constant reaction temperature (100 °C) were considered (see Methodology).

2. Model description

The Eulerian thermokinetic hydrochemical code KIRMAT (Gérard et al., 1998) has been developed from the single-reaction path model KINDIS (Madé et al., 1994), by using its geochemical formulation and its numerical method to solve chemical equations.

The thermokinetic geochemical code KINDIS was developed from the purely thermodynamic code DISSOL (Fritz, 1975; Fritz and Tardy, 1976; Fritz, 1981), which in turn originated from PATH1 (Helgeson et al., 1970). Theoretical kinetic rate laws for mineral dissolution and precipitation based on the Transition State Theory (TST) have been implemented in DISSOL. These geochemical codes have been intensively numerically tested and used in published studies on hydrothermal, diagenetic and weathering processes (e.g. Noack et al., 1993; Bertrand et al., 1994).

In KINDIS, the irreversible kinetic driving force is explicitly calculated and the sequence of partial equi-
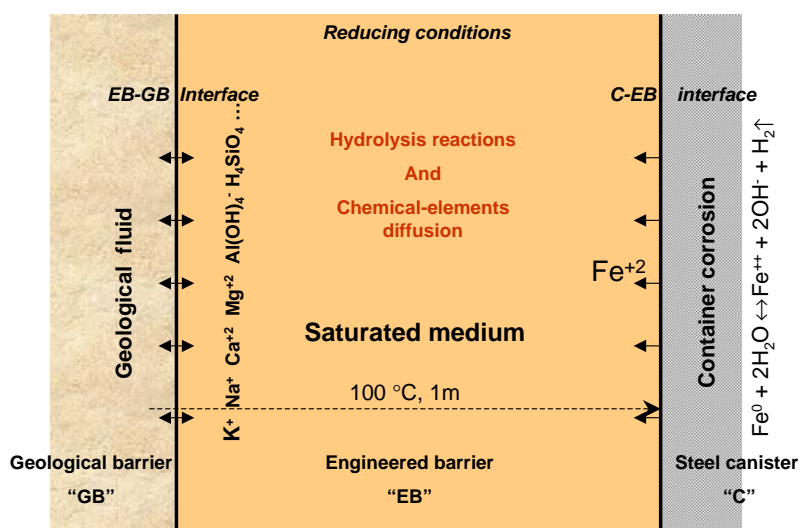

Fig. 2. Schematic representation of fluid–rock interaction and solute diffusion in an engineered barrier for radioactive waste confinement.

librium state is calculated from second-order Taylor series expansion (Madé et al., 1994).

In KIRMAT, solute transport is added to kinetic dissolution and/or precipitation reactions. A chemically controlled time step (noted Δt_c) allows preservation of accuracy of the calculations. Its value is inversely proportional to the largest of the first derivative variations among all the solute concentrations, and is controlled by setting the θ parameter (inversely proportional to Δt_c). The set of partial differential equations is integrated along one direction using the classical finite difference approximation method. An explicit scheme and a one-step algorithm are used to simultaneously solve the chemical (from KINDIS) and the conservative transport mass balance equations. A classical mixing cell scheme, the explicit-backward discretization, is computed for a numerical validation study.

The coupling of chemical reactions with mass transport is currently reported in the literature. Unfortunately it is still difficult to take into account all physico-chemical phenomena in a system (Steefel and Lasaga, 1990; Poinssot et al., 1998; Collin et al., 2002; Gens et al., 2002; Keijzer et al., 1999; Malusis and Shackelford, 2002; Ulm et al., 2002; Le Gallo et al., 1998; Savage et al., 2002; Hökmark et al., 1997; Carnahan, 1992; Kälvenius and Ekberg, 2003; Linklater et al., 2005 and others).

3. Methodology

3.1. General considerations

The following aspects were considered to simplify the modelling system.

(i) Geochemical transformations in a fluid-saturated medium.

A recent study showed that a bentonite barrier is fully water-saturated within approximately 3–4 years after deposition (Hökmark, 2004). This allows to assume that after the fluid-saturation phase, the engineered barrier is saturated with a fluid slightly concentrated with major chemical elements. In the present study, the engineered barrier is initially saturated with pure water because the interacting-fluid in the laboratory experiments to study the geochemical transformations, are regularly carried out with pure water. Obviously, the pure water as an interacting fluid with engineered barrier is a drastic consideration because the modeling system will be very reactive in the first years. In

consequence, the geochemical processes could be overestimated. The influence of interacting fluid concentration was not considered in the current study.

(ii) Solute diffusion.

In the water-saturated engineered barrier of bentonite, the interstitial fluid is almost static because of the very low permeability in the medium. In these conditions the convection transport can be negligible. Then, the significant transport phenomenon through the engineered barrier is uniquely the diffusion of chemical elements, mainly iron diffusion toward the geological medium, and K, Ca, Mg, Na, Si, etc. diffusion toward the metallic container.

(iii) Reducing conditions.

Following the closure of the repository system, the hydrolysis reactions of the mineral constituents "of the engineered barrier" take place in reducing conditions ($P_{O_2} \cong 0$; Eh $= -200$ mV) because the oxygen is rapidly consumed by corrosion of iron container (ex. $2Fe^0 + O_2 + 2H_2O \leftrightarrow 2Fe^{++} + 4OH^-$).

(iv) Container corrosion.

The container corrosion was considered as a dissolution reaction of metallic iron in reducing conditions:

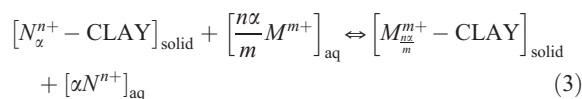$$Fe^0 + 2H_2O \Leftrightarrow Fe^{++} + 2OH^- + H_2 \uparrow . \tag{1}$$
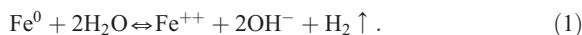
This perturbation into the system was simulated by a standard kinetic equation of mineral dissolution where the rate constant of iron dissolution was estimated considering a linear rate of corrosion of 5 [μm/year]. This assumption is based on the recent experimental results published by Idemitsu et al. (2002) and Xia et al. (2005); they estimated that the corrosion rate of carbon steel lies between 0.1 and 20 [μm/year] depending on the experimental conditions. The rate constant of iron dissolution was then estimated using the following formula:

$$k_{dFe} = \frac{v_{corrosion} \cdot \rho}{\bar{M}}, \left[mol / \left(m^2 \cdot year \right) \right] \tag{2}$$

with $v_{corrosion}$ the rate linear corrosion, ρ the specific (grain) density and $\bar{M}$ the molar mass of iron.

(v) Cation exchange process.

The KIRMAT code is based on the hydrolysis reactions, but the cation exchange process into the clays can be implicitly simulated by coupling of the dissolution–precipitation reactions. For this case, the interlayer charge of the transformed and/or neo-formed mineral phase (phyllosilicate or clay) must be conserved (i.e., the tetrahedral and octahedral charge of phyllosilicate remains constant). The formulation of cation exchange reaction can be represented by

$$\left[N_\alpha^{n+} - CLAY \right]_{solid} + \left[\frac{n\alpha}{m} M^{m+} \right]_{aq} \Leftrightarrow \left[M_{\frac{n\alpha}{m}}^{m+} - CLAY \right]_{solid}$$
$$+ \left[\alpha N^{n+} \right]_{aq} \tag{3}$$

where N and M are the exchangeable cations, CLAY represents a functional group of the clay-exchanger, n and m are the electrical charges of the exchangeable cations, α is the structural coefficient of interlayer cation, and solid and aq refer to the exchanger phases and aqueous solution, respectively.

3.2. Calculation of the swelling capacity decay

The calculation of the swelling capacity decay is based on the following equation (Montes-H et al., 2005):

$$D = \left(1 - \frac{V_{\text{d\_swell-clay}}}{V_{\text{i\_system}}}\right) + \frac{\sum V_{\text{p\_swell-clay}}}{V_{\text{i\_system}}} \quad (4)$$

where $V_{\text{d\_swell-clay}}$ is the volume of transformed swelling-clay, $V_{\text{p\_swell-clay}}$ is the volume of neo-formed swelling-clay, and $V_{\text{i\_sytem}}$ is the initial volume of swelling-clay in the system.

This simple equation allowed thus the estimation of the decay of swelling capacity by a volume balance, considering that the decay of swelling capacity is directly proportional to the volume of transformed montmorillonite (cation exchange + geochemical transformations) and, taking into account that it may be partially compensated by the volume of neo-formed swelling clays.

3.3. Input data

3.3.1. Primary minerals

MX80 bentonite has been widely studied by Sauzeat et al. (2001), Guillaume (2002), Montes-H (2002), Montes-H et al. (2003a,b), Montes-H and Geraud, 2004, Tournassat et al. (2003), Neaman et al. (2003), and others. The mineral composition of this material is presented in Table 1. In the present study, the minerals contained in the MX80 bentonite were considered as primary minerals or as reactants of any

possible mineral dissolution (or chemical transformation). This process was simulated by a standard kinetic equation (see Section 3.3.8). In contrast, their precipitation was considered as a thermodynamic equilibrium process (local equilibrium assumption).

3.3.2. Secondary minerals

The secondary minerals or neo-formed mineral phases were chosen following the conclusions of the laboratory experiments conducted at 80 and 300 °C, in the presence of metallic iron (Guillaume, 2002; Lantenois, 2003; Perronnet, 2004). In addition, it was supposed that the initial Na/Ca-montmorillonite contained in the bentonite barrier can be chemically exchanged with Ca^{+2}, Mg^{+2}, Na^+, K^+ and Fe^+. Table 2 presents the secondary minerals considered in the KIRMAT simulations. The precipitation (or neo-formation) of secondary minerals was considered as a thermodynamic equilibrium process (i.e. equilibrium condition for precipitation). For the future, it will be necessary to consider a kinetic process for mineral precipitation and/or crystallization of new phases in order to simulate a most realistic system.

3.3.3. Initial composition of fluid

The engineered barrier was considered as a saturated medium, initially saturated with pure water. In contrast, the geological fluid was a representative geological fluid of the French Callovo-Oxfordian Formation (see Table 3).

3.3.4. Temperature of reaction

In the KIRMAT code, it is not possible to take into account the temperature gradient as a function of time–space produced by the disintegration reactions of radioactive wastes. However, it is possible to take into account any temperature between 0 and 300 °C. The confinement barrier is subjected to temperature variations (>70 °C and some-

Table 1

Mineral composition of MX80 bentonite (after Sauzeat et al., 2001); and thermodynamic equilibrium constants used in KIRMAT simulations

Mineral	Volume fraction (dry bentonite)	Volume fraction water-saturated bentonite	Chemical formula	Log (km) (100 °C)
Pyrite	0.00313	0.002023	FeS_2	-67.89 [b]
Calcite	0.00966	0.006245	$CaCO_3$	-9.39 [b]
Quartz	0.07032	0.045465	SiO_2	-3.12 [b]
Microcline	0.01066	0.006892	$KAlSi_3O_8$	-18.17 [b]
Albite	0.03490	0.022564	$NaAlSi_3O_8$	-16.36 [b]
Biotite	0.02783	0.017993	$K(Fe_3)[Si_3AlO_{10}](OH)_2$	5.91 [b]
Na/Ca-montmorillonite	0.84350	0.898814	$[Si_{3.98}Al_{0.02}O_{10}](OH)_2$ $(Al_{1.55}Mg_{0.28}Fe_{0.09}^{III}Fe_{0.08}^{II})$ $(Na_{0.18}Ca_{0.10})$	-25.59 [a]
Total	1.00000	1.000000		

(a) Method based on the electronegativity scale (Vieillard, 2000).
(b) Data base of KIRMAT code.

Table 2
Secondary minerals and the thermodynamic equilibrium constants used in KIRMAT simulations

Mineral	Chemical formula	Log(km) (100 °C)
Saponite_332	$[(Si_{3.67}Al_{0.33}O_{10})(OH)_2](Al_{0.33}Fe^{II}_{1.15}Mg_{1.52})$	−1.81 [a]
Saponite Fe(II)	$[(Si_{3.67}Al_{0.33}O_{10})(OH)_2](Fe^{II}_3)Na_{0.33}$	6.93 [a]
Saponite_341	$[(Si_{3.5}Al_{0.5}O_{10})(OH)_2](Al_{0.25}Fe^{II}_{1.25}Mg_{1.5})Ca_{0.05}Na_{0.15}$	1.72 [a]
Vermiculite_170	$[(Si_{3.19}Al_{0.81}O_{10})(OH)_2](Al_{0.08}Fe^{III}_{0.295}Mg_{2.61}Fe^{II}_{0.015})Mg_{0.218}$	5.51 [a]
Na-montmorillonite	$[Si_{3.98}Al_{0.02}O_{10}(OH)_2](Al_{1.55}Mg_{0.28}Fe^{III}_{0.09}Fe^{II}_{0.08})Na_{0.38}$	−25.18 [a]
Ca-montmorillonite	$[Si_{3.98}Al_{0.02}O_{10}(OH)_2](Al_{1.55}Mg_{0.28}Fe^{III}_{0.09}Fe^{II}_{0.08})Ca_{0.19}$	−25.21 [a]
Mg-montmorillonite	$[Si_{3.98}Al_{0.02}O_{10}(OH)_2](Al_{1.55}Mg_{0.28}Fe^{III}_{0.09}Fe^{II}_{0.08})Mg_{0.19}$	−25.79 [a]
K-montmorillonite	$[Si_{3.98}Al_{0.02}O_{10}(OH)_2](Al_{1.55}Mg_{0.28}Fe^{III}_{0.09}Fe^{II}_{0.08})K_{0.38}$	−25.53 [a]
Fe-montmorillonite	$[Si_{3.98}Al_{0.02}O_{10}(OH)_2](Al_{1.55}Mg_{0.28}Fe^{III}_{0.09}Fe^{II}_{0.08})Fe_{0.19}$	−25.29 [a]
Phillipsite Na	$[Si_{10}Al_6O_{32}]Na_5Ca_{0.5}12H_2O$	−71.54 [b]
Laumontite	$[SiAl_2O_8]Ca4H_2O$	−24.63 [b]
Chabazite Na	$[Si_8Al_4O_{24}]Na_{3.5}Ca_{0.25}13H_2O$	−50.9 [b]
Greenalite	$Fe^{II}_3Si_2O_5(OH)_4$	17.43 [d]
Cronstedtite	$Fe^{II}_2Fe^{II}_2SiO_5(OH)_4$	12.18 [d]
Chamosite-7Å	$Fe^{II}_2Al_2SiO_5(OH)_4$	−11.0 [d]
Chrysotile	$Mg_3Si_2O_5(OH)_4$	24.5 [d]
Chlorite FeAl	$[Si_2Al_2O_{10}(OH)_2](Fe^{II}Al_2)(Fe^{II}_3)(OH)_6$	−28.05 [c]
Chlorite MgAl	$[Si_2Al_2O_{10}(OH)_2](MgAl_2)(Mg_3)(OH)_6$	−11.74 [c]
Illite	$[(Si_{3.5}Al_{0.5}O_{10})(OH)_2](Al_{1.8}Mg_{0.25})K_{0.6}$	−35.23 [b]
Goethite	$FeO(OH)$	9.35 [e]
Siderite	$FeCO_3$	−11.95 [e]
Hematite	α-Fe_2O_3	20.75 [e]
Magnetite	Fe_3O_4	22.65 [b]
Anhydrite	$CaSO_4$	−6.26 [b]
Gypsum	$CaSO_4 \cdot 2H_2O$	−5.16 [b]
Thenardite	Na_2SO_4	−0.879 [b]
Jarosite	$KFe^{III}_3(SO_4)_2(OH)_6$	−15.6 [b]
Cristobalite	SiO_2	−2.7 [d]
Amorphous silica	SiO_2	−2.25 [b]

(a) Method based on the electronegativity scale (Vieillard, 2000).
(b) Database of KIRMAT code.
(c) Method based on the electronegativity scale (Vieillard, 2002).
(d) Database of EQ36 code.
(e) Data compilation by Chivot, 2004.

times >100 °C) (Collin et al., 2002). In the present study, a constant temperature of 100 °C as a function of time–space was assumed. This unrealistic assumption allows to evaluate a drastic effect in the engineered barrier, i.e. the chemical transformations and/or the neo-formation of mineral phases are overestimated in the system.

3.3.5. Initial pH and P_{CO_2}

P_{CO_2} was initially fixed at 3.16×10^{-4} bar. Knowing that the alkaline reserve is close to zero for pure water, the initial pH was calculated at 5.89 considering a temperature of 100 °C.

3.3.6. Water–rock ratio

The total physical porosity of MX80 bentonite was estimated at 30% for an initial physical density of 1.7 g/cm³ (Sauzeat et al., 2001). Assuming that the engineered barrier was initially saturated with pure water and knowing that the KIRMAT code was based on 1 kg of water (i.e. approximately 1000 cm³ "V_{water}"), it is possible to calculate the volume of rock involved in the interaction (approximately 2333 cm³). This value, the mineral volume fraction of the dry bentonite, and the swelling potential of Na/Ca-montmorillonite, allow the calculation of the initial volume of each primary mineral in the system.

3.3.7. Thermodynamic equilibrium constants

The KIRMAT code is based on hydrolysis reactions where the major aqueous species are mainly H_4SiO_4, $Al(OH)_4^-$, CO_3^{2-}, SO_4^{2-}, Na^+, K^+, Ca^{2+}, Mg^{2+}, Fe^{2+}, Fe^{3+}, H^+ and H_2O. The thermodynamic equilibrium constants of

Table 3
Chemical composition, pH and Eh of a representative geological fluid from Callovo-Oxfordian formation (Jacquot, 2002)

Chemical parameters	Value	Observation
Eh [mV]	-176	SO_4/pyrite equilibrium
pH	7.30	Electroneutrality condition
Na [mol/kg H_2O]	3.2×10^{-2}	Na–Ca exchange
K [mol/kg H_2O]	7.1×10^{-3}	K–Ca exchange
Ca [mol/kg H_2O]	1.5×10^{-2}	Equilibrium with calcite
Mg [mol/kg H_2O]	1.4×10^{-2}	Na–Mg exchange
SiO_{2aq} [mol/kg H_2O]	9.44×10^{-5}	Equilibrium with quartz
Cl [mol/kg H_2O]	8.9×10^{-2}	Calculated by lixiviation
SO_4 [mol/kg H_2O]	3.40×10^{-3}	$pCO_2 = 3.09*10^{-3}$ condition
Al [mol/kg H_2O]	8.6×10^{-9}	Equilibrium with illite
Fe [mol/kg H_2O]	9.4×10^{-5}	Equilibrium with daphnite
C_T(Inorganic) [mol/kg H_2O]	1.3×10^{-3}	Equilibrium with dolomite
pCO_2 [atm]	$3.09*10^{-3}$	–

the hydrolysis reactions used in KIRMAT simulations at 100 °C are presented in Tables 1 and 2.

3.3.8. Kinetic data

The simplified equation used to simulate the dissolution rate of a mineral m in the KIRMAT code may be written as:

$$v_{dm}^s = k_{dm}^{pH} S_m^{eff} a_{H+}^n \left(1 - \frac{Q_m}{K_m} \right) \qquad (5)$$

where k_{dm}^{pH} is the constant of the apparent dissolution rate intrinsic to mineral m at a given pH [mol/m²/year]; S_m^{eff} is the effective or reactive surface area (as a function of the number of actives sites) at the mineral/aqueous solution interface [m²/kg H_2O]; a_{H+}^n is the activity of the H^+ ions in the aqueous solution, where n is a real exponent with a generally positive value in acid solutions, zero in neutral

solutions and negative in basic solutions; $(1 - Q_m/K_m)$ is the saturation index of mineral m in an aqueous solution, where Q_m is the ionic activity product and K_m is the thermodynamic equilibrium constant known for the given temperature and pressure conditions.

The intrinsic constant of mineral dissolution (k_{dm}^{pH}) is a function of the temperature, which can be described by the Arrhenius law:

$$k_{dm}^{pH} = A_m \cdot \exp\left(\frac{-E_{am}}{R.T} \right) \qquad (6)$$

with A_m being the frequency factor and E_{am} the activation energy of the mineral dissolution reaction [J/mol].

The k_{dm}^{pH} data used in the current study were taken from studies by Jacquot (2000) and Kluska (2001). These values are summarized in Table 4.

Conversely, the effective or reactive surface area (S_m^{eff}) could be defined as a percentage of the total mineral surface area, generally between 50% and 90% (White and Peterson, 1990). Recently, the atomic force microscopic experiments showed that only 8–14% of the total mineral surface area participate as reactive surface area (S_m^{eff}) in the dissolution of several silicates (Nagy et al., 1999; Tournassat et al., 2003). It is still difficult to estimate with precision the reactive surface area of silicates and phyllosilicates. Granular studies show that a bulk sample of MX80 bentonite is composed by 86.1% of particles <2 μm in size, 8.8% in the 2–50 μm range and 5.1% >50 μm (Neaman et al., 2003). In the present study, it was supposed (which is not really true) that the MX80 bentonite was composed of particles of 2 μm in size. This consideration simplified the calculation of the total mineral surface area (S_m^T) for each primary mineral. Finally, it was also assumed that only 10% of the total mineral surface area participated as reactive surface area ($S_m^{eff} = 0.1 S_m^T$). Evidently, these

Table 4
The kinetic data used in the KIRMAT simulations

Mineral	S_m^{eff} (*)		k_{dm}^{pH} [mol/m².year]		pH limit	
	[m²/kg H_2O]	k^H (*)	k^{H2O} (*)	k^{OH} (*)	A-to-N	N-to-B
Pyrite	2.19	1.88×10^{-18}	1.88×10^{-18}	1.88×10^{-18}	–	–
Calcite	6.76	7.93×10^6	8.69×10^2	8.69×10^2	4.4	8.3
Quartz	49.22	4.5×10^{-3}	1.7×10^{-3}	3.18×10^{-6}	2	5.5
Microcline	7.46	1.40	7.89×10^{-3}	5.97×10^{-6}	4.5	7.8
Albite	24.42	1.40	7.89×10^{-3}	5.97×10^{-6}	4.5	7.8
Biotite	19.48	1.34×10^{-3}	1.89×10^{-5}	5.45×10^{-7}	5	7
Montmorillonite	590.4	1.34×10^{-3}	1.89×10^{-5}	5.45×10^{-7}	5	7

k^H: constant of the dissolution rate in an acid medium.
k^{H2O}: constant of the dissolution rate in a neutral medium, independent of the pH.
k^{OH}: constant of the dissolution rate in a basic medium.
S_m^{eff}: reactive surface area.
A: acid; N: neutral; B: basic.
*kinetic data (after the compilations Jaquot, 2000 and Kluska, 2001).

assumptions are rough, but, this estimation of reactive surface area of mineral phases is still discussed in the literature.

The kinetic data (k_{dm}^{pH}, S_m^{eff}) used in the KIRMAT simulations are presented in Table 4.

3.3.9. Diffusion coefficient

The transport of solutes into the clay barrier was considered to be a pure diffusion process in a saturated medium. The coefficient of molecular diffusion tested in the simulations was 10^{-11} m^2/s. This value was selected based on published data for compacted MX80 (Lehikoinen et al., 1996). The KIRMAT code uses the same value for all chemical species.

4. Results and discussion

4.1. Chemical transformations in the bentonite barrier

A recent modelling study on the bentonite/iron/fluid interaction by Montes-H et al. (2005) has shown that the Na/Ca-montmorillonite-to-Ca-montmorillonite conversion was the most significant chemical transformation into the bentonite barrier under specific conditions of repository. This chemical process was interpreted to be a simple cation exchange reaction but the interlayer charge of montmorillonite was not considered constant in the chemical formula (see Table 3 in the paper, Montes-H et al., 2005). In addition, only two exchangeable cations (Ca^{+2}, Na^+) were taken into account. As this is an oversimplification, the present study specifies the assumptions by using the Eq. (3) and taking five exchangeable cations (Ca^{+2}, Mg^{+2}, Fe^{+2}, Na^+, K^+) into account (see Table 2).

In the following paragraphs, the chemical processes of Na/Ca-montmorillonite in the engineered barrier under repository conditions are described based on temporal–spatial graphical representations.

(1) Chemical behaviour of Na/Ca-montmorillonite.

It is clear that the physicochemical performance of MX80 bentonite barrier is directly linked to the chemical behaviour of initial Na/Ca-montmorillonite
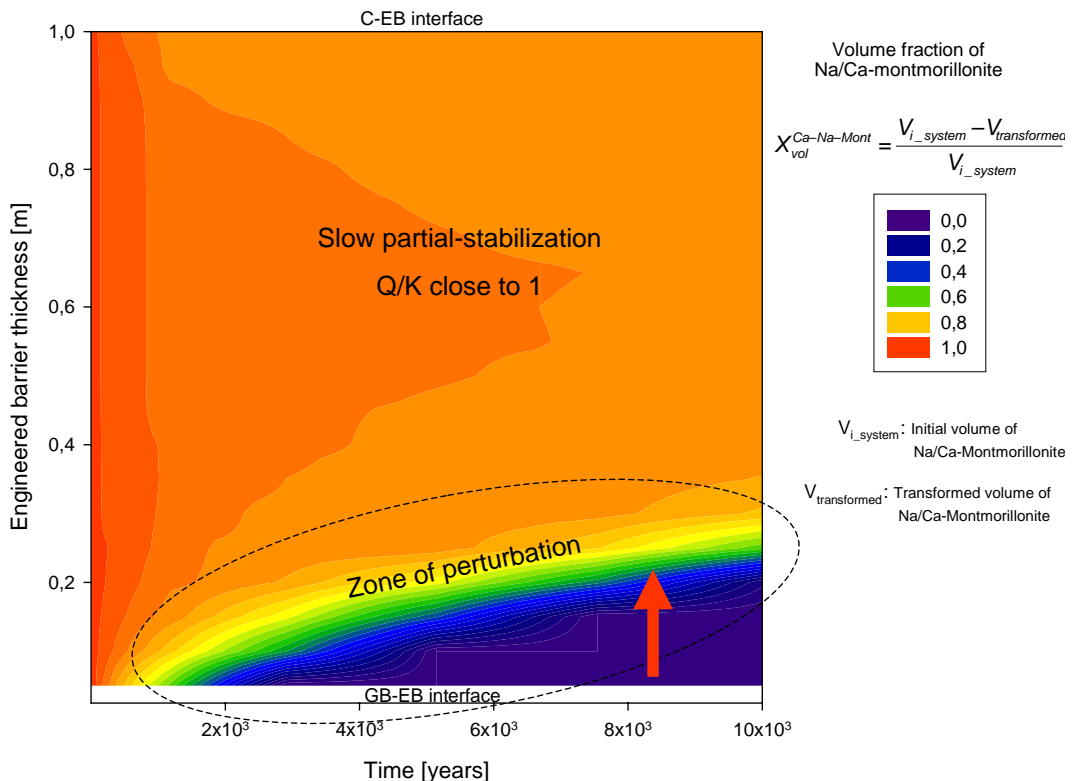

Fig. 3. Temporal and spatial chemical transformation of Na/Ca-montmorillonite into the MX80 bentonite barrier.
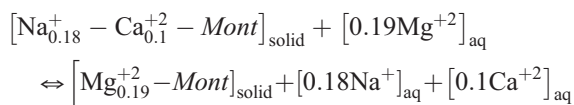
because it is main component (up to 85%) of the mineral assemblage. In the current study, a slow partial-stabilization of Na/Ca-Montmorillonite with the interacting fluid was reached (Q/K close to 1) (see Fig. 3). However, the system is constantly perturbed by canister corrosion within the C–EB interface and by diffusion of major elements within the GB–EB interface. The latter for example produces a significant chemical transformation of Na/Ca-montmorillonite into the bentonite barrier (Fig. 3). But, the chemical stability of Na/Ca-montmorillonite is highly dependent on thermodynamic equilibrium constants of secondary minerals. For example, a simple adjustment for Ca-montmorillonite (logK=−25.79) and Fe-montmorillonite (logK=−25.79) (see Table 2) increases the transformation rate of Na/Ca-montmorillonite and the partial stabilization of this clay with the interacting fluid was not observed.

(2) Cation exchange process.

Two main comments are given for this process.

First, the Na/Ca-montmorillonite is preferentially exchanged with Mg^{++} (Mg-montmorillonite) because the calculated thermodynamic-equilibrium constant for Mg-montmorillonite is more stable than Na, K, Ca and Fe-montmorillonites (see Table 2). Using the Eq. (3), this chemical process can be represented by the following reaction:

$$\left[Na_{0.18}^{+} - Ca_{0.1}^{+2} - Mont\right]_{solid} + \left[0.19Mg^{+2}\right]_{aq}$$
$$\Leftrightarrow \left[Mg_{0.19}^{+2} - Mont\right]_{solid} + \left[0.18Na^{+}\right]_{aq} + \left[0.1Ca^{+2}\right]_{aq}$$

where *Mont* represents the octahedral and tetrahedral layer, or the functional group of the montmorillonite-exchanger.

In order to avoid a preferential chemical stability, the Mg, Ca and Fe-montmorillonites were tested with the same thermodynamic equilibrium constant (logK=−25.79). For this case, the initial Na/Ca-montmorillonite was preferentially exchanged to Ca-mon-
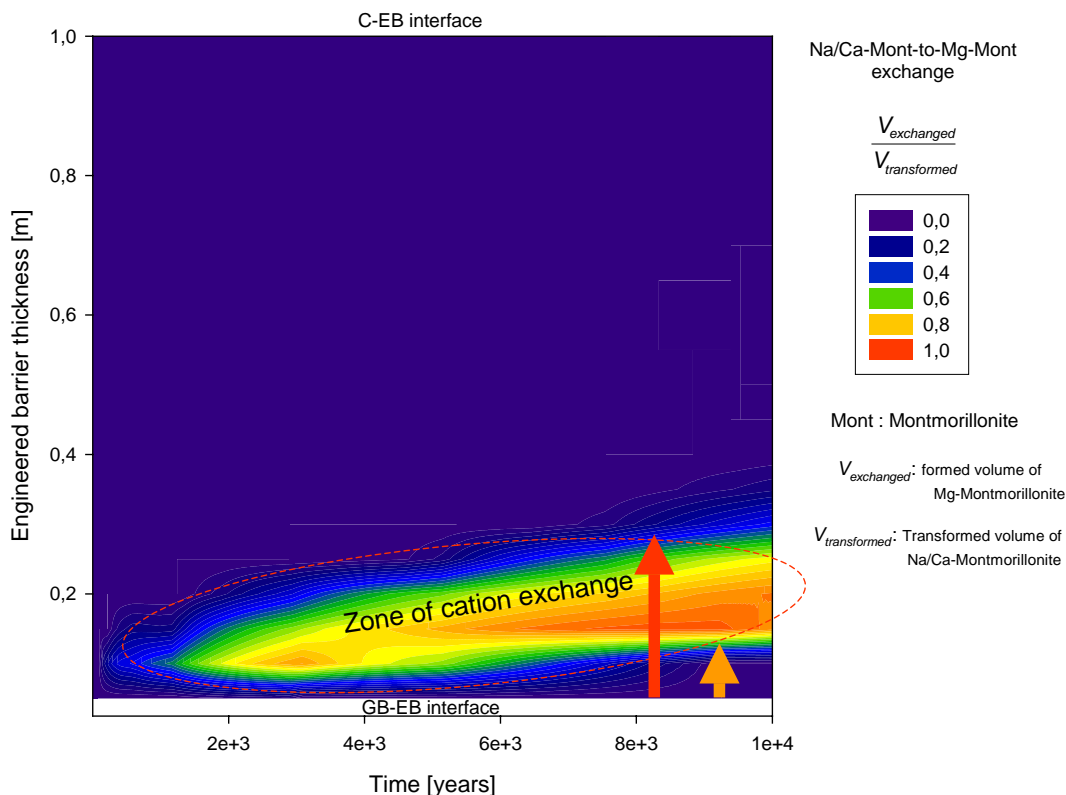

Fig. 4. Temporal and spatial Na/Ca-montmorillonite-to-Mg-montmorillonite exchange into the MX80 bentonite barrier.
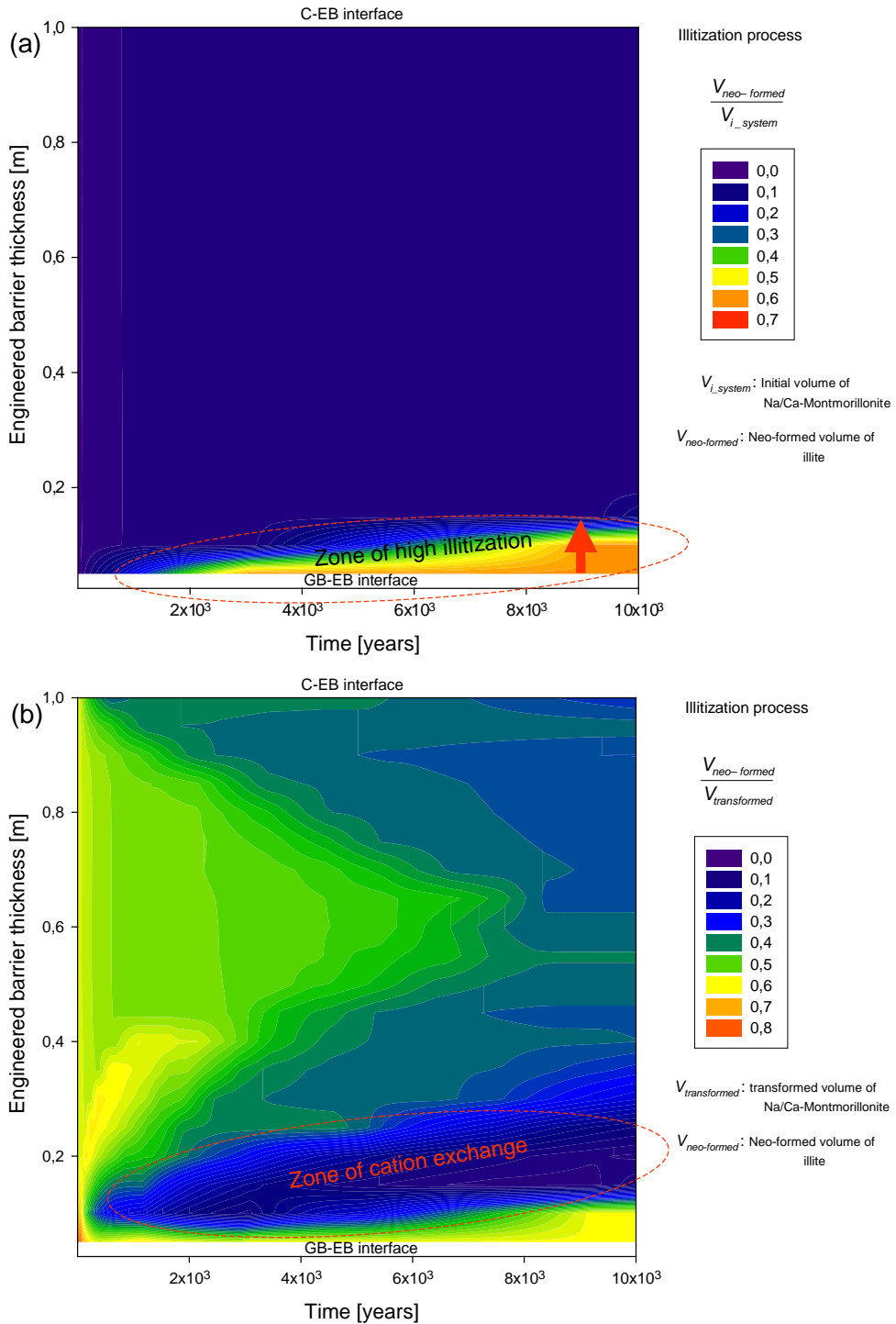
Fig. 5. a. Temporal and spatial illite neo-formation into the MX80 bentonite barrier. b. Temporal and spatial Na/Ca-montmorillonite-to-illite conversion into the MX80 bentonite barrier.

tmorillonite. That means that the cation concentration in the interacting fluid controls the cation exchange process. The Na/Ca-montmorillonite-to-Ca-montmor-illonite exchange was also identified in a previous modelling study (see Montes-H et al., 2005).

Second, the Na/Ca-Mont-to-Mg-Mont exchange is a potential chemical process in the bentonite barrier, especially adjacent to the GB–EB interface, which leads to the careful interpretation that the cation exchange is favoured by diffusion of major elements (see Fig. 4). Nevertheless, experimental studies and other modelling studies suggest that the Na/Ca-mon-tmorillonite-to-Ca-montmorillonite exchange to be the dominant process in the bentonite barrier. Fig. 4 shows that the cation exchange is diffused and displaced in the time–space. In fact, this chemical process seems to be a previous stage to the neo-formation of other mineral phases.

(3) Illitization process.

The illitization process is a potential chemical process for a bentonite barrier in the radioactive

waste repository because of relatively high potassium concentrations in the geological fluid (Hökmark et al., 1997; Guillaume, 2002). In addition, the chemical dissolution of the potassium bearing minerals microcline and biotite (both contained in the MX80 bentonite) could favour this process because additional potassium is available. Fig. 5a shows clearly that a high illitization process dominates adjacent to the GB–EB interface and is less significant with distance. This observation confirms that illitization process is controlled by the concentration–diffusion gradient of potassium that is contained in the geological fluid. It is important to remark that the role of thermal gradient close to the container interface was not considered in this study. Fig. 5b shows that the illitization process is also linked to the intensity of chemical transformation of Na/Ca-montmorillonite. However, it is limited by the cation exchange process because the $V_{\text{neo-formed}}/V_{\text{transformed}}$ ratio is relatively low in the zone of cation exchange. Finally, the chemical dissolution of microcline and biotite
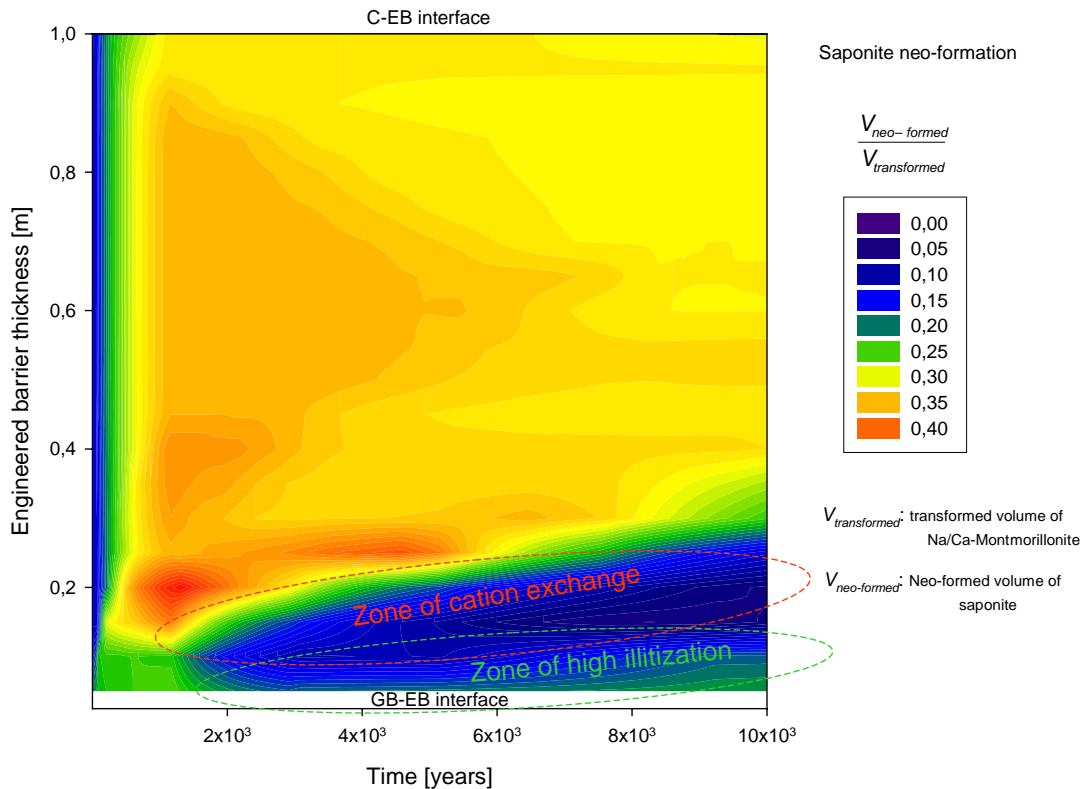

Fig. 6. Temporal and spatial saponite neo-formation into the MX80 bentonite barrier.

contributes slightly on the illitization in the bentonite barrier.

(4) Saponites neo-formation.

The saponite neo-formation is also considered to be a potential chemical process in a bentonite barrier for the radioactive waste repository due to the chemical transformation of montmorillonite (Guillaume, 2002). In the present study it was identified that the saponite neo-formation decreases with increasing cation exchange and illitization processes (see Fig. 6). If these chemical processes are not predominant, the saponite neo-formation depends directly on the chemical transformation of Na/Ca-montmorillonite (see Fig. 6).

5) Montmorillonite-to-zeolite conversion.

The montmorillonite-to-zeolite conversion is frequently regarded as a possible chemical transformation in bentonite barrier for the radioactive waste repository. For example, in laboratory experiments, zeolite group minerals were identified (Guillaume, 2002) within a closed system at 300 °C, but this temperature is far from the expected one. Thus in this study three tectosilicates were tested (see Table 2) and only the laumontite was shown to precipitate. This process seems to be favoured by the corrosion canister (see Fig. 7). This mineral phase is not a neo-formation and frequently identified as a transient phenomenon while the Na/Ca-montmorillonite-to-Ca-montmorillonite exchange takes place in the system.

6) Montmorillonite-to-chlorite conversion and neo-formation of ferrous phases.

The montmorillonite-to-chlorite conversion is also considered to be a potential chemical process in bentonite barrier for the radioactive waste repository because of a significant iron concentration in the geological fluid (Table 3) and the liberation of iron from the canister corrosion. In the present study, two chlorites at 14 Å and four iron-rich serpentines phases at 7 Å were tested (see Table 2). The results show a minimal neo-formation of a ferrous chlorite at 14 Å, which does not correspond to the recent experiments because the chlorites at 14 Å are neo-formations at temperatures over 100 °C (Guillaume, 2001).
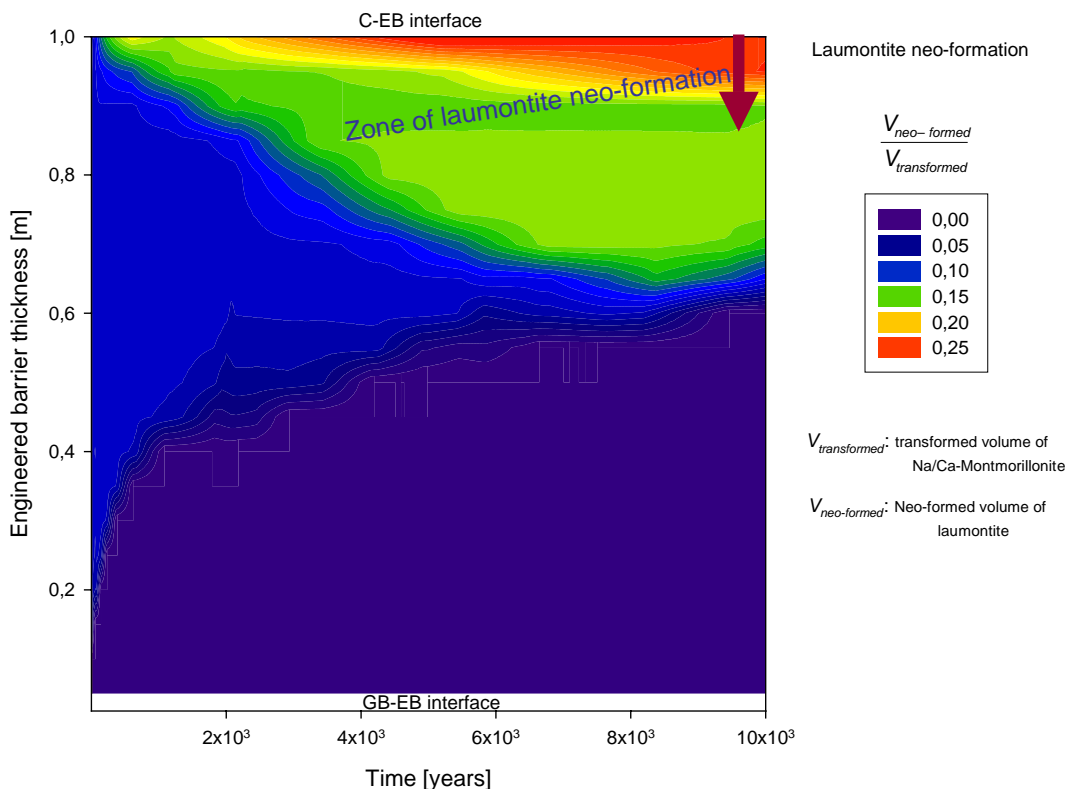

Fig. 7. Temporal and spatial laumontite neo-formation into the MX80 bentonite barrier.

Minor amounts of magnetite, as another neo-formed ferrous phase, were observed under reducing conditions preferentially near the C–EG interface which is quite typical (ex. Xia et al., 2005).

4.2. Final state of the bentonite barrier

Fig. 8 compares the initial state with the final state of the engineered barrier (EB) after 10,000 years of diffusion–reaction. This modelling study
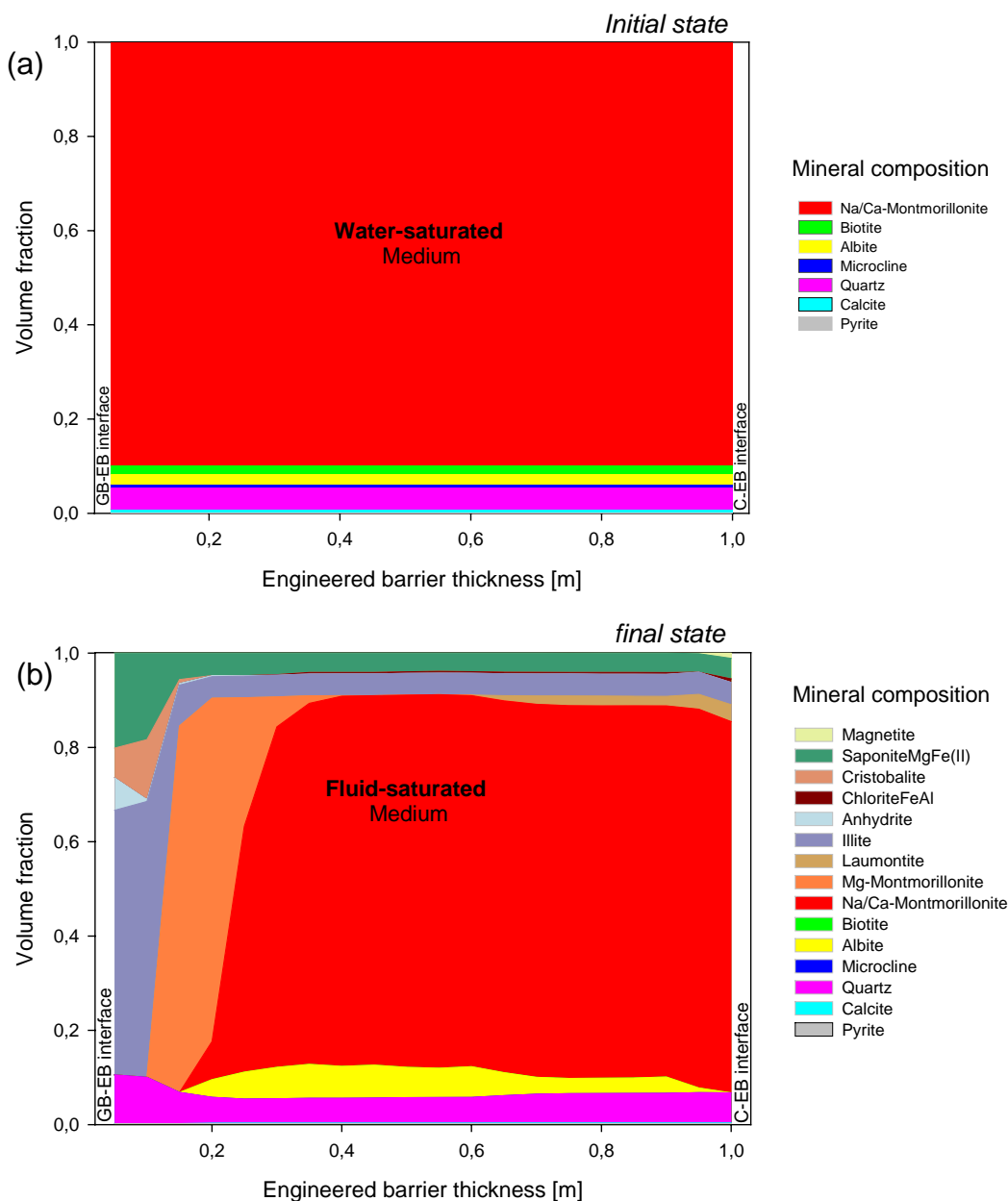

Fig. 8. a. Mineral composition of the engineered barrier at water-saturated conditions (initial state). b. Mineral composition of fluid-saturated engineered barrier after 10,000 years of diffusion-reaction (final state).

G. Montes-H et al. / Applied Clay Science 30 (2005) 181–198

demonstrates that the EB is highly transformed in contact with the geological fluid. The most significant chemical processes are illitization, cation exchange and saponization, which extend up to 20 cm significantly into the EB (see Fig. 8b). Less dominant chemical transformations in the EB were identified, such as a minimal neo-formation of silicates (quartz, cristobalite), anhydrite, laumontite, magnetite and chlorite.

4.3. Simplified method to evaluate the decay of swelling capacity

A simplified method based on volume balance (see Eq. (4)) shows that the swelling capacity of the bentonite barrier is slightly affected after 10,000 years of diffusion-reaction (D close to 1); because the volume of neo-formed swelling-clays is almost directly proportional to the volume of transformed Na/Ca-montmorillonite, except for a strong illitization and/or neo-formation of non-swelling clays. In the present study, this simple approach predicted that the decay of swelling capacity of the engineered barrier is drastically affected close to the geological barrier-engineered barrier interface. Out this zone the swelling capacity decay lies between 5% and 11% (see Fig. 9).

4.4. Physicochemical changes in the interacting fluid

(1) pH and Eh behaviour.

Fig. 10 shows a heterogeneous temporal–spatial behaviour of pH in the interacting fluid of engineered barrier. For example, a slightly acid pH was observed near the geological medium boundaries after 10,000 years. This decrease in pH could be due to a significant $[H^+]$ accumulation in the system, produced by neo-formation of saponites. In addition, the pH is poorly buffered in the system because initial volume fraction of calcite is low in the bentonite ($X_{\text{calcite}}=0.00624$, see Table 1). A sensitivity study on initial volume fractions of calcite showed that with higher fractions ($X_{\text{calcite}}>0.015$) the pH would be buffered efficiently in the system.

On the other hand, Fig. 10 shows a slight increase of pH (up to 6) in the interacting fluid of EG adjacent to container, for this case, the acidification process is partially compensated by the $[OH^-]$ diffusion (see Eq. (1)).

In general, there is a linear correlation between pH and oxidation–reduction potential (Eh). As the

$$D = \left(1 - \frac{V_{d\_swell-clay}}{V_{i\_system}}\right) + \frac{\sum V_{p\_swell-clay}}{V_{i\_system}}$$

D: Swelling capacity decay
$V_{p\_swell-clay}$: The volume of neo-formed swelling-clay
V_{i_sytem}: Initial volume of Na/Ca-montmorillonite
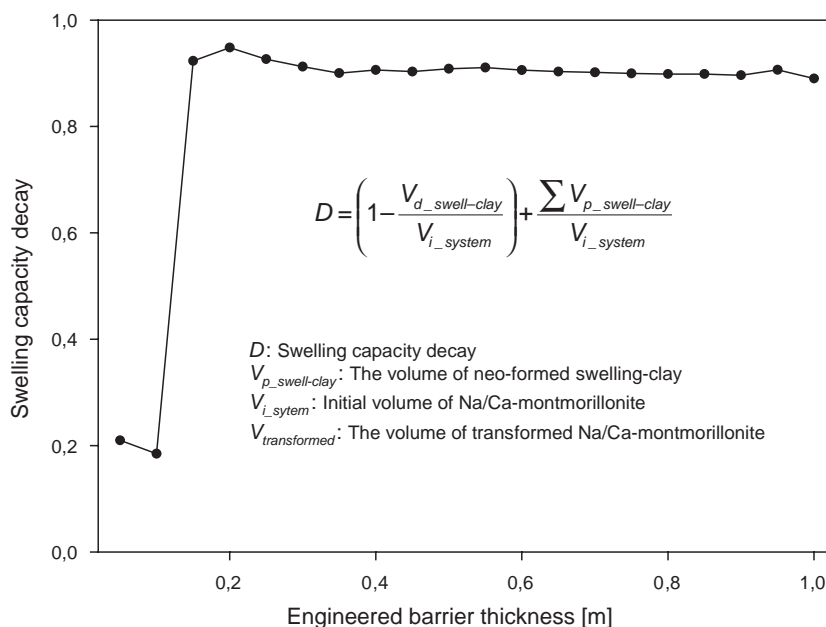$V_{transformed}$: The volume of transformed Na/Ca-montmorillonite

Fig. 9. Swelling capacity decay of the engineered barrier after 10,000 years of diffusion-reaction.
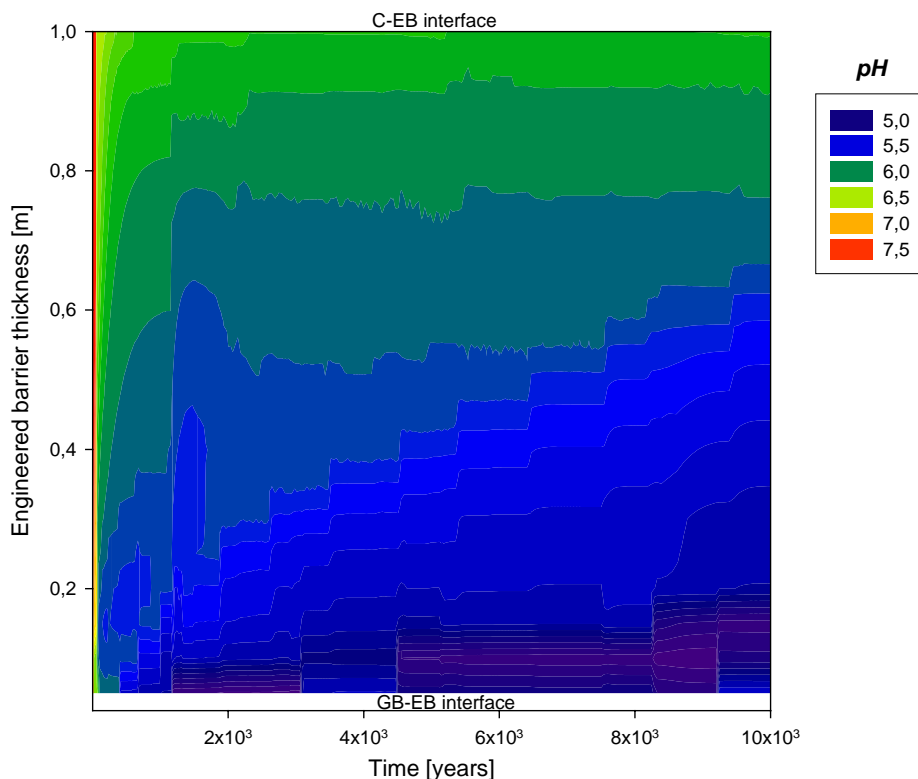
Fig. 10. Temporal and spatial pH evolution of the interacting fluid into the engineered barrier.

correlation is inversely proportional, the oxidation–reduction potential decreases with increasing pH and vice versa. For example, the interacting fluid of the engineered barrier presents after 10,000 years of diffusion–reaction the reducing properties most significant close to iron canister (Eh $\cong -215$ mV) whereas the Eh of interacting fluid is close to -120 mV adjacent to geological barrier.

(2) chemical-elements composition.

High dissolution of the bentonite is manifested by the increased Si, Al, Mg, K, Ca and Na contents in the interacting fluid.

A significant concentration in iron [Fe^{2+}] in the interacting fluid indicates a slight neo-formation of chlorites and the other ferrous mineral phases in the system. This phenomenon is controlled by the silicate mineral dissolution and the corrosion of iron-container.

A significant concentration in potassium in the interacting fluid suggests the illitization to be a potential process in the system.

4.5. Uncertainty sources

The chemical transformations occurring in a bentonite barrier for radioactive waste confinement depend directly on the reaction temperature, the rate of iron corrosion, the composition of the interacting fluid, the nature and/or amount of accessory minerals, the diffusion coefficients of solutes, the reactive surface area of minerals, the thermodynamic constants of minerals, the texture of porous media, etc. At the present time, it is difficult to efficiently consider all parameters in the same model because of the complexity of their estimation. Consequently, the KIRMAT simulations were carried out under the drastic conditions found in a radioactive waste repository:

1. There was an infinite source and constant concentration of major cations in the boundaries of the geological medium.

2. The temperature of reaction, reactive surface area of minerals, diffusion coefficients of solutes and porosity were considered to remain constant in time and space.

In the present study, a key input parameter contributing to modelling uncertainty is the reactive surface area because this parameter strongly influences the kinetic of dissolution. It is clear that the reactive surface area does not correspond to the measured physical surface area of the material; unfortunately, it is still difficult to estimate the reactive surface area of silicates and phyllosilicates with precision.

Another input parameter that could contribute significantly to uncertainty in this modelling study is the selection of appropriate secondary minerals to be included in the simulation and the specific thermo-dynamic data used to define their solubility. For phyllosilicates, the equilibrium constants are rarely available in the literature and their estimation is based on theoretical methods.

5. Conclusion

The KIRMAT modelling code showed a good performance to simulate the chemical transformations (geochemical and cation exchange reactions) coupled with chemical-elements diffusion into the engineered barrier under repository conditions.

The results showed that the EB in contact with the geological fluid was highly transformed after 10,000 years, whereas the most significant chemical processes were illitization, cation exchange and saponization, extending up to 20 cm into the EB. Chemical transformations of minor importance in the EB were identified as well, such as a neo-formation of silicates (quartz, cristobalite), anhydrite, laumontite, magnetite and chlorite in the system.

A simplified method based on volume balance showed that the swelling capacity of the bentonite barrier is slightly affected after 10,000 years of diffusion–reaction (D close to 1) because the volume of neo-formed swelling-clays is almost directly proportional to the volume of transformed Na/Ca-montmorillonite, except for a strong illitization and/or neo-formation of non-swelling clays. In the present study, this simple approach predicted that the decay of swelling capacity of the engineered barrier is drastically affected close to the geological barrier-engineered barrier interface. Out this zone the swelling capacity decay lies between 5% and 11%.

Acknowledgement

References

Bertrand, C., Fritz, B., Sureau, J.-F., 1994. Hydrothermal experiments and thermo-kinetic modelling of water–sandstone interactions. Chemical Geology 116, 189–202.

Carnahan, C.L., 1992. Numerical simulation of heterogeneous chemical reactions coupled to fluid flow in varying thermal field. Scientific Basis For Nuclear Waste Management XV, Mat. Res. Soc. Symp. Proc., vol. 257, pp. 683–690.

Chivot, J., 2004. Thermodynamique des produits de corrosion. Fonctions thermodynamiques, diagrammes de solubilité, diagrammes E-pH des systèmes Fe-H_2O, Fe-CO_2-H_2O, Fe-S-H_2O, Cr-H_2O et Ni-H_2O en fonction de la température. Collection Sciences and TechniquesANDRA. 141 pp.

Collin, F., Li, X.L., Radu, J.P., Chalier, R., 2002. Thermo-hydromechanical coupling in clay barriers. Engineering Geology 64, 179–193.

Fritz, B., 1975. Etude themodynamique et simulation des réactions entre minéraux et solutions. Application à la géochimie des altérations et des eaux continetales. Mémorie di Scienze Géologiche 41 (Strasbourg, France, 153 pp.).

Fritz, B., 1981. Etude thermodynamique et modélisation des réactions hydrothermales et diagénétiques. Mémorie di Scienze Géologiche 65, 197.

Fritz, B., Tardy, Y., 1976. Séquence de minéraux secondaires dans l'altération des granites et roches basiques: modèles thermodynamiques. Bulletin de la Société Géologique de France 18, 7–12.

Gens, A., Guimaraes, L.do.N., Garcia-Molina, A., Alonso, E.E., 2002. Factors controlling rock–clay buffer interaction in a radioactive waste repository. Engineering Geology 64, 297–308.

Gérard, F., Clement, A., Fritz, B., 1998. Numerical validation of a Eulerian hydrochemical code using a 1D multisolute mass transport system involving heterogeneous kinetically controlled reactions. Journal of Contaminant Hydrology 30, 201–216.

Guillaume, D., 2002. Etude expérimentale du système fer-smectite en présence de solution à 80 °C et 300 °C. PhD Thesis, Henri Poincaré University, Nancy I, France, 210 pp.

Helgeson, H.C., Brown, T.H., Nigrini, A., Jones, T.A., 1970. Calculations of mass transfer in geochemical processes involving aqueous solutions. Geochimica et Cosmochimica Acta 34, 569–592.

Hökmark, H., 2004. Hydration of the bentonite buffer in a KBS-3 repository. Applied Clay Science 26, 219–233.

Hökmark, H., Karnland, O., Pusch, R., 1997. A technique for modeling transport/conversion processes applied to smectite-to-illite conversion in HLW buffers. Engineering Geology 47, 367–378.

Idemitsu, K., Yano, S., Xia, X., Inagaki, Y., Arima, T., Mitsugashira, T., Hara, M., Suzuki, Y., 2002. Diffusion behavior of iron corrosion products in buffer materials. Materials Research Society Symposia Proceedings 713, 113–120.

Jacquot, E., 2000. Modélisation thermodynamique et cinétique des réactions géochimiques entre fluides de bassin et socle cristallin. PhD Thesis, Louis Pasteur University, Strasbourg I, France, 202 pp.

Jacquot, E., 2002. Composition des eaux interstitielles des argilites du Callovo-Oxfordien non perturbées. Rapport ANDRA No. D NT ASTR 02-041, 13 pp.

Kälvenius, G., Ekberg, C., 2003. TACK-a program coupling chemical kinetics with a two-dimensional transport model in geochemical systems. Computers Geosciences 29, 511–521.

Keijzer, Th.J.S., Kleingeld, P.J., Loch, J.P.G., 1999. Chemical osmosis in compacted clayey material and the prediction of water transport. Engineering Geology 53, 151–159.

Kluska, J.M., 2001. Modélisation Thermodynamique et Cinétique des Réactions Géochimiques dans une Barrière Ouvragée en Bentonite. Simulations dans des conditions réductrices, de 60 à 180 °C en l'absence et en présence d'une source de fer sur une durée de 20 ans. RapportANDRA. (No. CRP 0CGS 01-004, 34 pp.)

Kluska, J.M., Fritz, B., Clement, A., 2002. Predictions of the mineralogical transformations in a bentonite barrier surrounding an iron radioactive container. International Meeting "Clay in Natural and Engineered Barriers for Radioactive Waste Confinement", 8–12 December 2002, Reims, France. ANDRA.

Komine, H., 2004. Simplified evaluation for swelling characteristics of bentonites. Engineering Geology 71, 265–279.

Komine, H., Ogata, N., 2003. New equations for swelling characteristics of bentonite-based buffer materials. Canadian Geotechnical Journal 40, 460–475.

Lantenois, S., 2003. Réactivité fer metal/smectites en milieu hydraté à 80 °C. PhD. Thesis, Orleans University, France, 188 pp.

Le Gallo, Y., Bildstein, O., Brosse, E., 1998. Coupled reaction-flow modelling of diagenic changes in reservoir permeability, porosity and mineral compositions. Journal of Hydrology 209, 366–388.

Lehikoinen, J., Carlsson, J., Muurinen, A., Olin, M., Salonen, P., 1996. Evaluation of factors affecting diffusion in compacted bentonite. Materials Research Society Symposia Proceedings 412, 675–682.

Linklater, C.M., Sinclair, D.J., Brown, P.L., 2005. Coupled chemistry and transport modelling of sulphidic waste rock dumps at the Aitik mine site, Sweden. Applied Geochemistry 20, 275–293.

Madé, B., Clément, A., Fritz, B., 1994. Modelling mineral/solution interactions: the thermodynamic and kinetic code KINDISP. Computers and Geosciences 20 (9), 1347–1363.

Malusis, M.A., Shackelford, C.D., 2002. Theory for reactive solute transport through clay membrane barriers. Journal of Contaminant Hydrology 59, 291–316.

Montes-H, G., 2002. Etude expérimentale de la sorption d'eau et du gonflement des argiles par microscopie électronique à balayage environnementale (ESEM) et analyse digitale d'images. PhD Thesis, Louis Pasteur University, Strasbourg I, France, 161 pp.

Montes-H, G., Geraud, Y., 2004. Sorption kinetic of water vapour of MX80 bentonite submitted to different physical–chemical and mechanical conditions. Colloids and Surfaces. A, Physicochemical Engineering Aspects 235, 17–23.

Montes-H, G., Duplay, J., Martinez, L., Mendoza, C., 2003. Swelling–shrinkage kinetics of MX80 bentonite. Applied Clay Science 22, 279–293.

Montes-H, G., Duplay, J., Martinez, L., Geraud, Y., Rousset-Tournier, B., 2003. Influence of interlayer cations on the water sorption and swelling–shrinkage of MX80 bentonite. Applied Clay Science 23, 309–321.

Montes-H, G., Fritz, B., Clement, A., Michau, N., 2005. A simplified method to evaluate the swelling capacity evolution of a bentonite barrier related to geochemical transformations. Applied Geochemistry 20, 409–422.

Nagy, K.L., Cygan, R.T., Hanchar, J.M., Sturchio, N.C., 1999. Gibbsite growth kinetics on gibbsite, kaolinite, and muscovite: atomic force microscopy evidence for epitaxy and assessment of reactive surface area. Geochimica et Cosmochimica Acta 63 (16), 2337–2351.

Neaman, A., Pelletier, M., Villieras, F., 2003. The effects of exchanged cations, compression, heating and hydration on textural properties of bulk bentonite and its corresponding purified montmorillonite. Applied Clay Science 22, 153–168.

Noack, Y., Collin, F., Nahon, D., Delvigne, J., Michaux, L., 1993. Secondary-mineral formation during natural weathering of pyroxene: review and thermodynamic approach. American Journal of Science 293, 111–134.

Perronnet, M. 2004. Réactivité des matériaux argileux dans un contexte de corrosion métallique. Application au stockage des déchets radioactifs en site argileux. Thèse INPL Nancy, 283 pp.

Poinssot, C., Toulhoat, P., Goffé, B., 1998. Chemical interaction between a simulated nuclear waste glass and different backfill materials under a thermal gradient. Applied Geochemistry 13 (6), 715–734.

Sauzeat, E., Guillaume, D., Neaman, A., Dubessy, J., François, M., Pfeiffert, C., Pelletier, M., Ruch, R., Barres, O., Yvon, J., Villéras, F., et Cathelineau, M., 2001. Caractérisation minéralogique, cristallochimique et texturale de l'argile MX80. RapportANDRA. No. CRP0ENG 01-001, 82 pp.

Savage, D., Noy, D., Mihara, M., 2002. Modelling the interaction of bentonite with hyperalkaline fluids. Applied Geochemistry 17, 207–223.

Steefel, C.I., Lasaga, A.C., 1990. Permeability changes due to coupled flow and reaction. In: Melchior, D.C., Basset, R.L. (Eds.), Chemical Modelling of Aqueous Systems II, Amer. Chem. Soc., Symp. Ser., vol. 416, pp. 212–216.

Tournassat, C., Neaman, A., Villiéras, F., Bosbach, D., Charlet, L., 2003. Nanomorphology of montmorillonite particles: estimation of the clay edge sorption site density by low pressure gas adsorption and AFM observations. American Mineralogist 88, 1989–1995.

Ulm, F.J., Heukamp, F.H., Germaine, J.T., 2002. Residual design strength of cement-based materials for nuclear waste storage systems. Nuclear Engineering and Design 211, 51–60.

Vieillard, P., 2000. A new method for the prediction of Gibbs free energies of formation of hydrated clay minerals based on the electronegativity scale. Clays and Clay Minerals 48 (4), 459–473.

Vieillard, P., 2002. A new method for the prediction of Gibbs free energies of formation of phyllosilicates (10Å and 14Å) based on the electronegativity scale. Clays and Clay Minerals 50 (3), 352–363.

White, A.F., Peterson, M.L., 1990. Role of reactive-surface-area characterization in geochemical kinetic models. In: Melchior, D., Bassett, R. (Eds.), Chemicals Modelling of Aqueous Systems II, Assoc. Chem. Soc. Symp. Series, vol. 416, pp. 461–475.

Xia, X., Idemitsu, K., Arima, T., Inagaki, Y., Ishidera, T., Kurosawa, S., Iijima, K., Sato, H., 2005. Corrosion of carbon steel in compacted bentonite and its effect on neptunium diffusion under reducing condition. Applied Clay Science 28, 89–100.